Infectious Disease Modelling 9 (2024) 1045–1056

Contents lists available at ScienceDirect

Infectious Disease Modelling

journal homepage: www.keaipublishing.com/idm

# Gonorrhea cluster detection in Manitoba, Canada: Spatial, temporal, and spatio-temporal analysis☆

Amin Abed [a, *], Mahmoud Torabi [a], Zeinab Mashreghi [b]

[a] Department of Community Health Sciences, University of Manitoba, Winnipeg, Manitoba, R3E 0W3, Canada
[b] Department of Mathematics and Statistics, University of Winnipeg, Winnipeg, Manitoba, R3B 2E9, Canada

ARTICLE INFO

*Article history:*
Received 1 November 2023
Received in revised form 23 May 2024
Accepted 25 May 2024
Available online 31 May 2024
Handling Editor: Dr Yijun Lou

*Keywords:*
Cluster detection
Gonorrhea
Infectious disease
Spatial analysis
Spatio-temporal analysis

ABSTRACT

In Canada, Gonorrhea infection ranks as the second most prevalent sexually transmitted infection. In 2018, Manitoba reported an incidence rate three times greater than the national average. This study aims to investigate the spatial, temporal, and spatio-temporal patterns of Gonorrhea infection in Manitoba, using individual-level laboratory-confirmed administrative data provided by Manitoba Health from 2000 to 2016. Age and sex patterns indicate that females are affected by infections at younger ages compared to males. Moreover, there is an increase in repeated infections in 2016, accounting for 16% of the total infections. Spatial analysis at the 96 Manitoba regional health authority districts highlights significant positive spatial autocorrelation, demonstrating a clustered distribution of the infection. Northern districts of Manitoba and central Winnipeg were identified as significant clusters. Temporal analysis shows seasonal patterns, with higher infections in late summer and fall. Additionally, spatio-temporal analysis reveals clusters during high-risk periods, with the most likely cluster in the northern districts of Manitoba from January 2006 to June 2014, and a secondary cluster in central Winnipeg from June 2004 to November 2012. This study identifies that Gonorrhea infection transmission in Manitoba has temporal, spatial, and spatio-temporal variations. The findings provide vital insights for public health and Manitoba Health by revealing high-risk clusters and emphasizing the need for focused and localized prevention, control measures, and resource allocation.



## 1. Introduction

Gonorrhea caused by Neisseria gonorrhoeae (specifically, the gonococcus) is a Sexually Transmitted Infection (STI)(-Whelan et al., 2021), and continues to be a significant global public health issue (Unemo et al., 2019). In Canada, Gonorrhea is the second most frequent STI, following Chlamydia (Choudhri et al., 2018; Lu et al., 2020). Gonorrhea is usually spread through unprotected vaginal, anal, or oral sexual interactions and results in cervicitis in women and urethritis in both men and women (Holmes et al., 2007; Schmale et al., 1969; Workowski, 2013). Moreover, transmission rates are higher from men

☆ This document is the results of the research project funded by Natural Sciences and Engineering Research Council of Canada (NSERC).
* Corresponding author.
*E-mail address:* Abeda@myumanitoba.ca (A. Abed).
Peer review under responsibility of KeAi Communications Co., Ltd.

https://doi.org/10.1016/j.idm.2024.05.009

to women compared to the reverse direction through vaginal intercourse (Walker and Sweet, 2011). Most of the infected men with gonococcal urethritis exhibit symptoms. However, fewer women with urogenital Gonorrhea manifest symptoms, and when they do, the symptoms lack specificity. Rectal and pharyngeal Gonorrhea are primarily detected in men who have sex with men (Bernstein et al., 2010). It is also common among women and often does not show any noticeable symptoms.

Microbiological diagnosis of Gonorrhea encompasses the culture of Gonorrhea, and/or the utilization of Nucleic Acid Amplification Tests (NAATs) (Lunny et al., 2015). NAATs provide increased sensitivity while upholding a strong degree of specificity. However, the sensitivity can differ among various NAATs and depending on the specific anatomical site being examined (Choudhri et al., 2018; Lunny et al., 2015; Unemo et al., 2013). Gonorrhea also plays a role in enhancing the transmission of the Human Immunodeficiency Virus (HIV) (Choudhri et al., 2018; Holmes et al., 2007; Unemo et al., 2019) and facilitating the propagation of other sexually transmitted infections (Unemo et al., 2019). Transmission of Gonorrhea infection can occur from infected mothers to their newborns during the birthing process (intrapartum). This is due to the vulnerability of the neonate's conjunctiva as it traverses the birth canal, potentially resulting in ophthalmia neonatorum if the conjunctiva becomes infected with Gonorrhea (Unemo et al., 2019). Additionally, infection during pregnancy is linked to outcomes like low birth weight and neonatal conjunctivitis, which can escalate and lead to vision impairment (Unemo et al., 2019; Vallely et al., 2021; World Health Organization, 2018).

In women, since Gonorrhea frequently persists without symptoms, it complicates the prompt identification and treatment of the infection (Davidson et al., 2021). Failure to detect and adequately treat infections can lead to ascending complications like epididymitis and salpingitis. This situation raises the likelihood of women developing cervicitis, pelvic inflammatory disease, ectopic pregnancy, and infertility (Choudhri et al., 2018; Holmes et al., 2007; Lenz & Dillard, 2018; Simms & Stephenson, 2000; World Health Organization, 2018). In men, asymptomatic Gonorrhea increases the probability of contracting epididymitis, epididymal-orchitis, chronic prostatitis, and infertility (Ochsendorf, 2008; Okonofua et al., 2022; Trojian et al., 2009; Wang et al., 2017). Increased vulnerability is attributed to various sexual practices, including irregular condom usage, engagement with multiple partners, and instances where a partner or partners maintain concurrent relationships (Choudhri et al., 2018; Holmes et al., 2007; World Health Organization, 2018). Certain populations are especially susceptible to infection. These include adolescents and young adults, specific ethnic and racial communities, socioeconomically disadvantaged groups, community of men who have sex with men, and sex workers (Leichliter et al., 2020). Gonorrhea has significantly been underestimated and not fully reported on a global scale even in high-income countries with established STI surveillance systems (World Health Organization, 2018). Annually reported Gonorrhea infections are estimated to represent only a fraction of the actual rates, with at least 70 percent going undetected or unreported (Choudhri et al., 2018; van Lier et al., 2016), primarily because these infections are often asymptomatic (Choudhri et al., 2018). While the asymptomatic nature of the infection partly explains this, underreporting is also due to delayed healthcare seeking and limited availability or inadequacy of Gonorrhea testing and treatment options (Leichliter et al., 2020; Whelan et al., 2021). Curable STIs including Gonorrhea do not establish robust and long-lasting protective immunity. After treating Gonorrhea, recurrent infection rates usually range from 10% to 20% (Hosenfeld et al., 2009; Bernstein et al., 2010).

Researchers identified a connection between areas with lower socioeconomic status and higher rates of Gonorrhea and Chlamydia infections in the health regions of Calgary, Canada (Bush et al., 2008). These areas were concentrated primarily in downtown and the northeastern part of the city. A study conducted in Manitoba, Canada, revealed that among cases of Gonorrhea and their associated contacts, the top 10% of relationships spanned distances of 237 km or more (Hippe & Jolly, 2012). Furthermore, this study found a higher proportion of long-distance partnerships among Gonorrhea cases compared to Chlamydia cases. Another study examined and compared the transmission patterns of Chlamydia and Gonorrhea in Winnipeg, Manitoba, Canada (Blanchard et al., 1998). Based on these results, the infections in both cases displayed high incidence rates that were concentrated in particular geographic areas characterized by lower socioeconomic status.

In 2017, the recorded annual incidence rate of Gonorrhea in Canada was 95.8 infections per 100,000 population. In 2018, Manitoba reported a significantly higher incidence of Gonorrhea, with a rate of 265 infections per 100,000 individuals. This sharp increase in rates exceeding the national average highlights the significant importance of Gonorrhea as a relevant and essential topic in the field of public health in Manitoba.

Our research aims to investigate the spatial, temporal, and spatio-temporal patterns of Gonorrhea infection in Manitoba. Manitoba province comprises a total of 96 Regional Health Authority Districts (RHADs). We utilize administrative data from 2000 to 2016 to identify RHADs and time periods with higher Gonorrhea incidence than what would be expected by chance. Therefore, the results of this study provide public health officials and decision-makers with a more comprehensive understanding of infection clusters and dynamics. The generated risk maps visually illustrate the geographical concentration of high-risk RHADs at different time periods, offering valuable insights for the implementation of targeted surveillance and more effective preventative strategies and control measures.

## 2. Materials and methods

### 2.1. Data sources

The Cadham Provincial Laboratory (CPL), operated by Manitoba Health, serves as the only public health laboratory in the province of Manitoba over three centuries and provides a diverse set of public health laboratory services. These services encompass areas such as the storage of testing data related to notifiable diseases, early detection of health risks, monitoring of

outbreak investigations, and the identification of disease causes. CPL is organized into different sections, comprising media/quality assurance, microbiology, perinatal chemistry, serology/parasitology, and virus detection. One of the responsibilities of the clinical microbiology section is to conduct investigations into STIs, including Gonorrhea. Gonorrhea infection is confirmed through laboratory tests like culture or NAAT. CPL is required to report all confirmed infections of Gonorrhea to the Epidemiology and Surveillance Unit, which operates within the Public Health Branch of the Manitoba Health (Lix et al., 2012). The unit's responsibility is to assist the public health system by actively monitoring, analyzing, and reporting on the occurrence, dissemination, and severity of both communicable and non-communicable diseases and their conditions in Manitoba.

In this study, we consider administrative health records of diagnosed infections of Gonorrhea in the province of Manitoba, Canada, from 2000 to 2016 provided by Manitoba Health. The individual-level data consists of sex, date of birth, date of diagnosis, 6-digit postal code of residence, and scrambled Personal Health Identification Numbers (PHINs) of confirmed Gonorrhea infections. The ICD-9-CM codes 098, V02, and V02.7 were utilized to identify Gonorrhea infections in the dataset.

### 2.2. Study area

Manitoba is divided into five Health Authority Districts (HADs): Interlake, Northern, Prairie, Southern, and Winnipeg. Within these HADs, there are a total of 96 RHADs, with specific numbers allocated to each HAD: 15 in Interlake, 16 in Northern, 17 in Prairie, 23 in Southern, and 23 in Winnipeg. (Fig. 1). This geographic classification algorithm has been defined by the Manitoba Centre for Health Policy (MCHP) and Manitoba Health for the allocation of HADs and RHADs based on municipality and postal codes. Using the geographic classification algorithm, we aggregate diagnosed Gonorrhea infections into 96 RHADs, which are then linked to 2016 Statistics Canada census data to obtain information on the sex, age, and population of residents in those RHADs.

### 2.3. Time series analysis

#### 2.3.1. Time series decomposition

A fundamental goal in the analysis of time series data involves breaking down a sequence into a collection of hidden components that are not directly observable. These components are linked to diverse forms of temporal changes. Time series data can encompass four primary kinds of fluctuations including trend or long-term tendency $T_t$, cyclical movements $C_t$, seasonal variations $S_t$, and irregular component, noise, or residual variations $I_t$. Therefore, considering an additive model, the time series $x_t$ can be conceptualized as $x_t = T_t + C_t + S_t + I_t$ while multiplicative model would be as $x_t = T_t \times C_t \times S_t \times I_t$. The seasonal index is computed by dividing the average number of infections for a specific month by the average monthly case count observed throughout the entire study period (West, 1997). This index approaching a value of 1.0 indicates that there are no clear and distinct seasonal patterns present in the data.

#### 2.3.2. Seasonal auto-regressive integrated moving average model

A time series comprises a sequence of numerical information collected at consistent time intervals over a specific duration. The Auto-Regressive Integrated Moving Average (ARIMA) model consists of three hyperparameters that specify the autoregressive (AR), integrated (I), and moving average (MA) components used to model the non-seasonal part of a time series. The ARIMA model is represented by ARIMA($p$, $d$, $q$), where $p$ is the order of the non-seasonal AR component, $d$ indicates the degree of differencing applied to the non-seasonal part by subtracting past values a certain number of times, and $q$ specifies the order of the non-seasonal MA component.

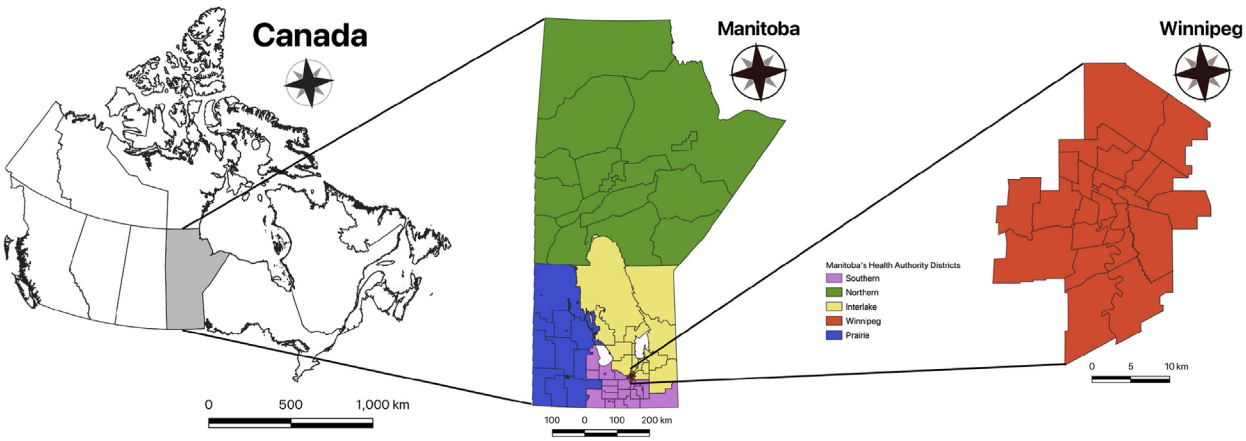


**Fig. 1.** Manitoba province with 5 HADs and 96 RHADs.

The Seasonal ARIMA (SARIMA) model is a broader version of the ARIMA model designed to explicitly accommodate univariate time series data featuring both a seasonal component and non-seasonal trends using a multiplicative approach (Box et al., 2015; Chan & Cryer, 2008; Faverjon & Berezowski, 2018). Seasonality involves a regular and repeating pattern within a dataset, usually following a specific time interval. The SARIMA model extends this concept, incorporating the three hyperparameters from the non-seasonal ARIMA($p$, $d$, $q$) model, along with additional hyperparameters that define the seasonal period (S). The model is denoted as SARIMA($p$, $d$, $q$)($P$, $D$, $Q$)$m$, where the initial three parameters ($p$, $d$, $q$) pertain to the non-seasonal aspect (the ARIMA model), while the latter parameters ($P$, $D$, $Q$)$m$ are associated with the seasonal aspect. More precisely, $P$ signifies the order of the seasonal AR component, $D$ indicates the level of differencing for the seasonal part, $Q$ denotes the order of the seasonal MA component, and $m$ represents the number of periods within each season. To predict the value of $x_t$ at time $t$ within a time series dataset $x_i$, $i = 0, \ldots, t-1$, the SARIMA model is employed and formulated as follows:

$$\left(1-\sum_{i=1}^{p}\varphi_i L^i\right)\left(1-\sum_{i=1}^{P}\Phi_i L^{im}\right)(1-L)^d\left(1-L^m\right)^D x_t = \left(1+\sum_{i=1}^{q}\theta_i L^i\right)\left(1+\sum_{i=1}^{Q}\Theta_i L^{im}\right)\epsilon_t,$$

where $Lx_t = x_{t-1}$ and $L^i x_t = x_{t-i}$ represent the lag operators, $\epsilon_t$ denotes the error terms, $\varphi_i$ and $\Phi_i$ represent the parameters of the non-seasonal and seasonal AR components, respectively, and $\theta_i$ and $\Theta_i$ denote the parameters of the non-seasonal and seasonal MA components, respectively.

### 2.4. Spatial and spatio-temporal clustering

#### 2.4.1. Spatial autocorrelation

Spatial autocorrelation, as measured by Global Moran's $I$ (Moran, 1950), serves as an indicator for analyzing spatial autocorrelation. The Global Moran's $I$ statistic falls within a range between $-1$ and 1. A Global Moran's $I$ statistic equal to 0 shows the absence of spatial autocorrelation, indicating a random distribution and no clustered districts across the entire study area. A value greater than 0 states the presence of positive spatial correlation, and when it approaches 1, it signifies a strong positive autocorrelation, indicating that districts are clustered. The significance of the Global Moran's $I$ statistic is assessed through the Monte Carlo test. This test helps determine whether the observed spatial autocorrelation is statistically significant or could have occurred by random chance. The interpretation of Global Moran's $I$ should be considered in the context of its null hypothesis. The null hypothesis specifies that the features are randomly distributed among the districts within the area under study. A $p$-value resulting from this test below the 5% significance level shows the existence of spatial autocorrelation among districts across the entire area under study. The Global Moran's $I$ statistic is given by:

$$I = \frac{N\sum_{i=1}^{z}\sum_{j=1}^{z} w_{ij}\left(x_i-\bar{x}\right)\left(x_j-\bar{x}\right)}{\left(\sum_{i=1}^{z}\sum_{j=1}^{z} w_{ij}\right)\sum_{i=1}^{z}\left(x_i-\bar{x}\right)},$$

where $N$ represents the total number of features, $z$ is the number of districts, $x_i$ and $x_j$ denote the number of features in district $i$ and $j$ respectively, $\bar{x}$ represents the mean value across the entire districts, and $w_{ij}$ represents the spatial weight between districts $i$ and $j$.

#### 2.4.2. Spatial and spatio-temporal scan statistics

Kulldorff's space–time scan statistic (Kulldorff, 1997) has been applied in diverse contexts within the field of epidemiology (Fukuda et al., 2005). Assume that the geographical area under study is divided into $z$ districts. The districts can be counties, enumeration districts, or health authorities. For each district $i$, consider $N_i$ as the number of infections with observed value $n_i$, $i = 1, \ldots, z$, and the total number of observed infections $n = \sum_{i=1}^{z} n_i$. The number of infections within each district follows a Poisson distribution with parameter $\psi_i\zeta_i$ (i.e., $N_i \sim \text{Poisson}(\psi_i\zeta_i)$, $i = 1, \ldots, z$), where $\psi_i$ and $\zeta_i$ denote the expected number of infections and the relative risk in district $i$, respectively. Consider the following hypothesis test

$$\begin{cases} H_0 : \mathbb{E}(N_i) = \psi_i, & \forall i \in \{1,\ldots,z\}, \\ H_1 : \mathbb{E}(N_i) > \psi_i, & \exists i \in \{1,\ldots,z\}, \end{cases} \tag{1}$$

where the null hypothesis states there is no clustering. The circular spatial scan statistic is a circular scanning window represented as $\omega$ and is applied to each centroid of $z$ districts shifted across the area under study. As a result, as the circular scanning window moves to different positions within the district, distinct sets of districts are included. For any given centroid, the radius of the circular scanning window changes smoothly, ranging from zero to a predetermined maximum distance, or up to a predetermined maximum count of $K$ districts that should be included within the cluster. Typically, the value of $K$ is selected to encompass a maximum of 50% of the population at risk. Hence, the circular scanning window is flexible both in distance and number of districts. If the circular scanning window contains the centroid of a district, then that whole district is included in the circular window. In total, a considerable quantity of distinct yet overlapping circular windows are generated.

Each circular scanning window possesses a unique position and size, representing a potential cluster candidate. Let $\omega_{ik}$ denote the circular window composed by the $(k-1)$-nearest neighbours to district $i$, for $k = 1, \ldots, K$ and $i = 1, \ldots, z$. Then, all the circular windows to be scanned by the spatial scan statistic are included in the set which is $\Omega = \{\omega_{ik} | 1 \leq i \leq z, 1 \leq k \leq K\}$. Therefore, the null and alternative hypotheses in (1) are expressed as

$$\begin{cases} H_0 & : \quad \mathbb{E}(N(\omega)) = \psi(\omega), & \forall \omega \in \Omega, \\ H_1 & : \quad \mathbb{E}(N(\omega)) > \psi(\omega), & \exists \omega \in \Omega, \end{cases}$$

where $N(\cdot)$ and $\psi(\cdot)$ denote the random variable for the number of infections and the null expected number of infections within the specified circular window, respectively. The alternative hypothesis $H_1$ states there is at least one window $\omega \in \Omega$ for which the underlying risk is higher inside the circular window when compared with outside. A likelihood of the observed count of infections both inside and outside the circular window can be calculated for every circular window $\omega \in \Omega$. Considering the Poisson assumption, the likelihood ratio for the specific circular window $\omega \in \Omega$ is given by:

$$\underset{\omega \in \Omega}{\mathcal{L}(\omega)} = \begin{cases} \left(\dfrac{n(\omega)}{\psi(\omega)}\right)^{n(\omega)} \left(\dfrac{n - n(\omega)}{n - \psi(\omega)}\right)^{n - n(\omega)}, & n(\omega) > \psi(\omega), \\ 1, & n(\omega) \leq \psi(\omega), \end{cases}$$

where $n(\omega)$ is the observed number of infections in the circular window $\omega \in \Omega$. The circular window $\omega^* \in \Omega$ that achieves the highest likelihood ratio is defined as the most likely cluster and is given by $\omega^* = \underset{\omega \in \Omega}{\arg\max}\ \mathcal{L}(\omega)$.

The scanning window takes on different shapes depending on the context. In spatial scanning, it typically manifests as a circular or elliptical shape. In temporal scanning, the scanning window represents a specific time span. However, in space-time scanning, the window adopts a cylindrical shape. Here, the cylinder's base symbolizes the spatial dimension, while its height corresponds to the temporal dimension.

As our study uses aggregated data based on RHADs, if the centroid of a RHAD falls within the radius of the circle associated with a specific RHAD, then that particular RHAD should be included as part of the window. Spatial and spatio-temporal clustering analysis of Gonorrhea infections are performed using the SaTScan™ software developed by Kulldorff (Kulldorff et al., 1998). *R* software version 4.3.1 is used for time series analysis, decomposing, and estimating the seasonal occurrences of monthly infections.

## 3. Results

### 3.1. Age and sex patterns

Fig. 2a presents the total and sex-specific annual incidence rates of reported infections per 100,000 population. It is evident that there is a significant increase in the annual rate of the infections for both sexes in 2016 when compared to preceding years. The data highlights a significant change in the sex distribution during the study period. From mid-2005 onwards, there is a shift in the sex distribution, as the rate of infections in females started to exceed that of males by an average of around 10 more infections per 100,000 population annually. This shift could be influenced by a combination of factors such as sexual behaviors factors, underreporting in males, asymptomatic infections, sexual network dynamics, and demographic changes. This trend in sex continues until the end of the study period in 2016, when a near balance happened, with nearly equal numbers of reported infections in both sexes. Fig. 2b also illustrates that the mean age of infected

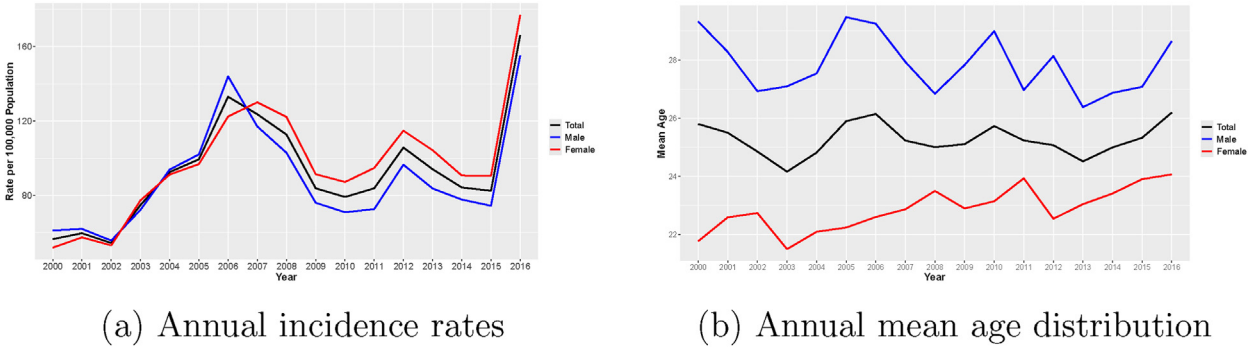


**Fig. 2.** Annual incidence rates (a) and age-sex distribution (b) of Gonorrhea infections in Manitoba, 2000–2016.

individuals is approximately 25 years. Moreover, there exists a notable sex-age disparity within the dataset. Specifically, the mean age for female cases hovered around 23 years, whereas for male cases, it is observed around 28 years. This divergence underscores a distinctive age-related pattern, with male cases presenting as roughly 5 years older than their female counterparts, thereby suggesting a propensity for Gonorrhea to manifest at younger ages among females. Furthermore, the analysis of mean age among both male and female cases as well as the overall mean age across the entire study period exhibit a consistent and stable pattern. No specific trend or significant deviation in mean age is observed over the duration of the study. This finding suggests that the infection's prevalence among different age groups remained relatively constant during the years under study.

Fig. 3 illustrates the annual rates of age and sex-specific age groups of reported Gonorrhea infections per 100,000 population, categorized into distinct age groups (0–14, 15–19, 20–24, 25–29, 30 and older). This graphical representation offers valuable insights into the prevalence and distribution of infections among various age groups. It enables a better understanding of how the infection affects different age and highlights potential sex disparities in its impact. This classification corresponds to the stages of development and milestones associated with sexual behavior. Adolescents usually start exploring their sexuality in their mid-teens (ages 15–19), and this trend of increased sexual activity and engagement in risky behaviors continues into early adulthood (ages 20–24 and 25–29) (Pinto et al., 2018; Unemo et al., 2019). This breakdown highlights important phases of sexual development and the potential risk of Gonorrhea exposure. Moreover, research consistently indicates that Gonorrhea infections typically peak during late adolescence and young adulthood, emphasizing the significance of these age groups for monitoring and intervention efforts (Cantos & del Rio, 2020; Unemo et al., 2019). By focusing on these peak transmission periods, public health authorities can allocate resources efficiently and implement targeted prevention strategies where they are most needed. In Fig. 3b, for instance, it is readily observable that a notable portion of annual rates of females occurs within the age group of 15–19, whereas annual rates of males primarily concentrated within the age group of 20–24.

Given access to the PHINs of infections, we were able to identify instances of repeat infections, denoting infections where individuals contracted more than once within a single year. To quantify the prevalence of repeated infections for each year, we computed the percentage by dividing the number of repeat infections by the total number of infections for that respective year. Fig. 4 presents a visual representation of the percentage of repeated infections in Manitoba from 2000 to 2016. This figure illustrates a significant rise in the percentage of reported infections in 2016, with approximately 16% of infections being linked to individuals who had multiple infections within the same year. This marks a substantial increase when compared to previous years. Additionally, from the second half of 2007 onward, there is a higher occurrence of recurrent infections among females compared to males.

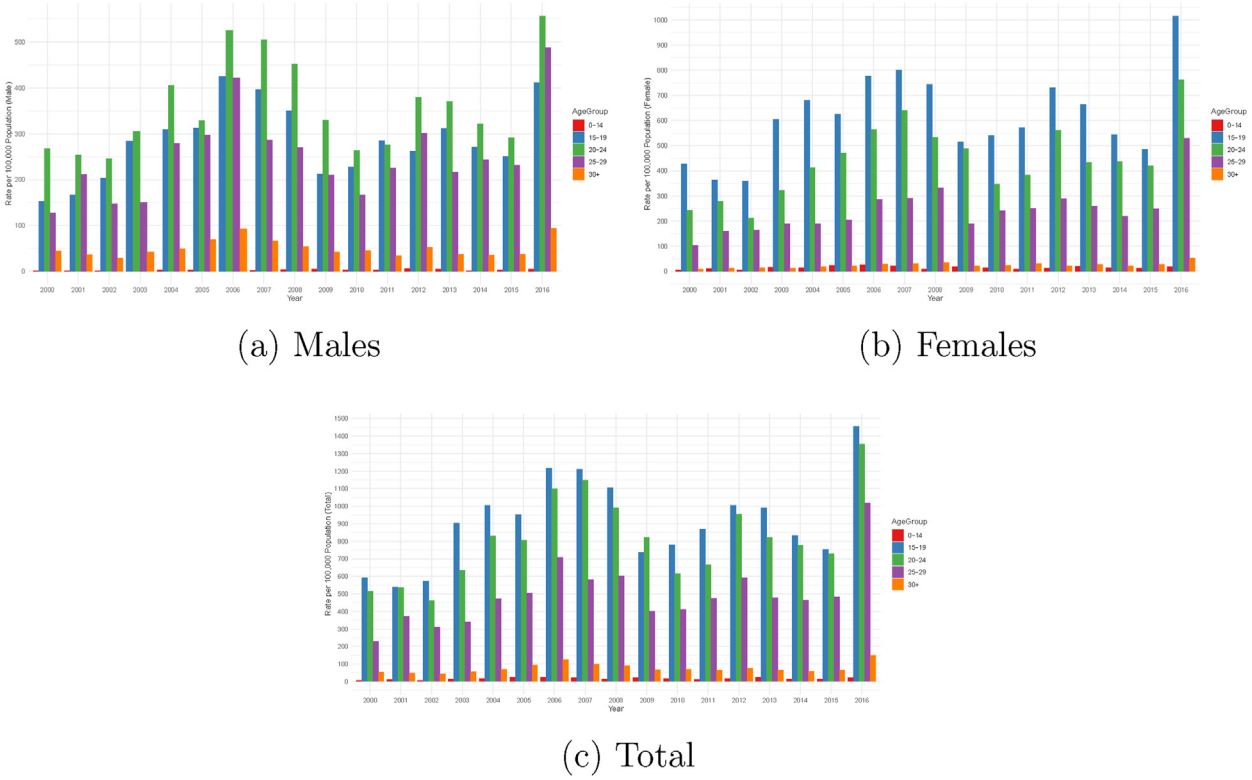


**Fig. 3.** Annual rates of age groups of reported Gonorrhea infections per 100,000 population in Manitoba, 2000–2016, for males (a), females (b), and total (c).

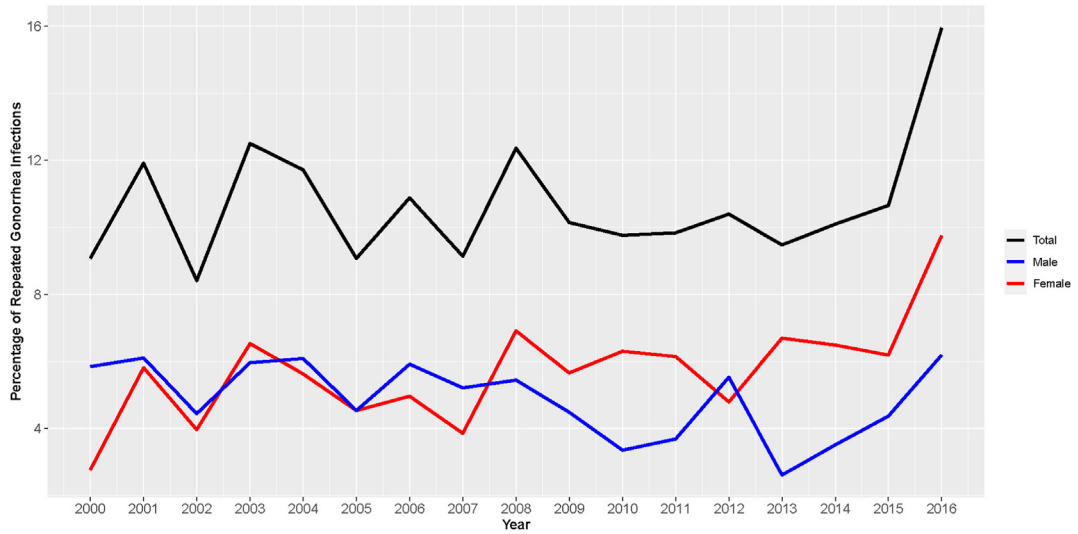


**Fig. 4.** Percentage of annually repeated Gonorrhea infections in Manitoba, 2000–2016.

### 3.2. Spatial patterns

The Global Moran's $I$ value of 0.48 ($p$-value $< 0.05$) suggests a statistically significant positive spatial autocorrelation of infections among the RHADs in Manitoba from 2000 to 2016. This indicates a non-random spatial clustered distribution of Gonorrhea infections.

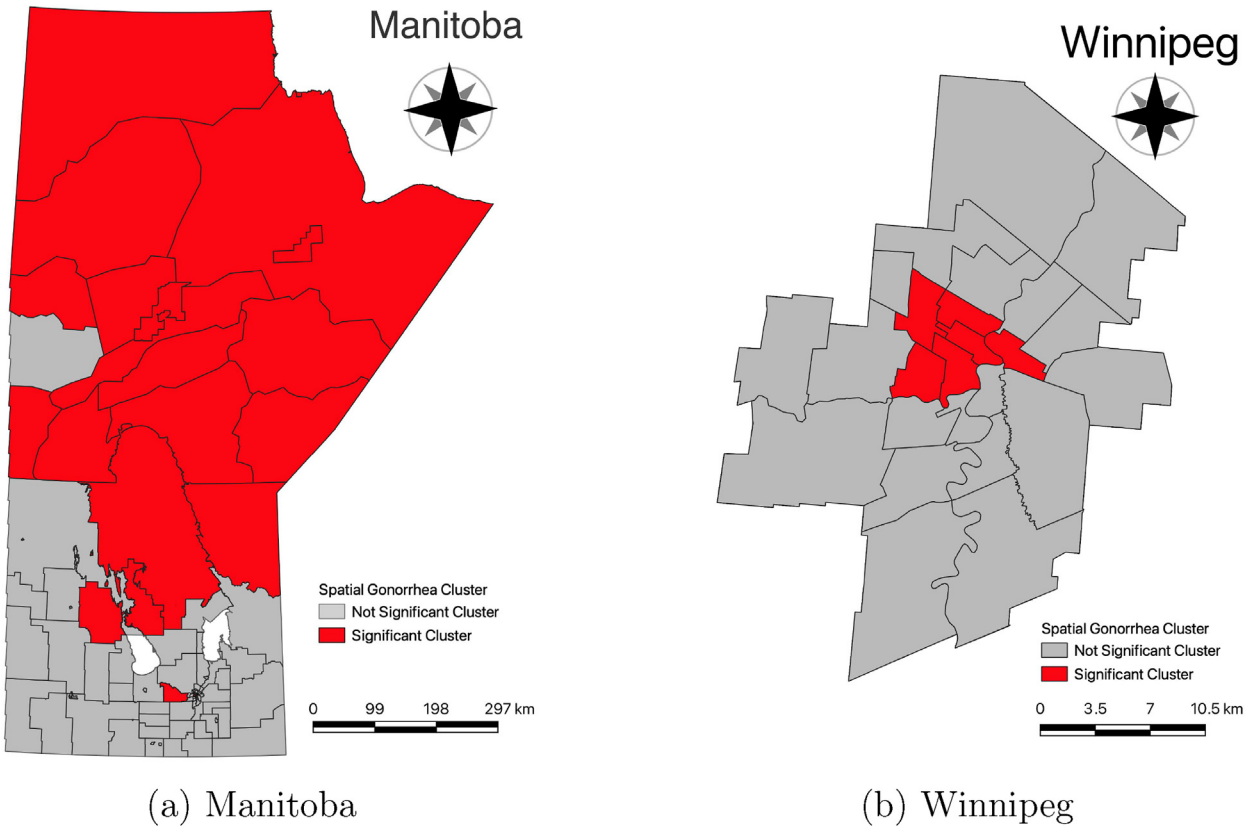


**Fig. 5.** Spatial clusters of Gonorrhea infections in Manitoba, 2000–2016.

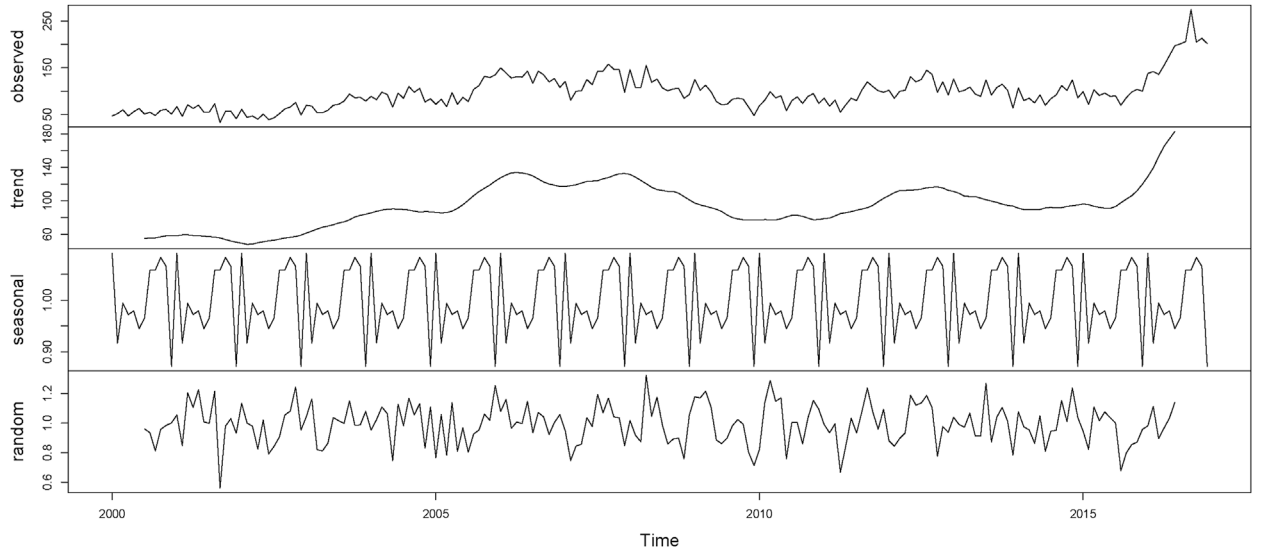


**Fig. 6.** Monthly time series data decomposition.

We aggregate the data of Gonorrhea infections for each RHAD ignoring temporal information. We adjust the expected number of cases for age groups (0–14, 15–19, 20–24, 25–29, 30 and older) and sex (male and female) using 2016 Statistics Canada census data of residence and population residing in the 96 RHADs for purely spatial analysis. We also consider a circular window scanning for a maximum of 50% of the total at-risk population. Kulldorff's space-time scan statistic, implemented using a discrete Poisson model within a purely spatial framework, results in the detection of 26 RHADs, as illustrated in Fig. 5. This indicates that the northern districts of Manitoba with 20 RHADs and the central districts of Winnipeg with 6 RHADs are significant clusters for the incidence of the infection.

### 3.3. Temporal patterns

As temporal information is not incorporated in our purely spatial analysis presented in Section 3.2, we intend to explore the temporal patterns of Gonorrhea in Manitoba. The annual incidence rates of infections exhibits cyclical fluctuations throughout the study period (Fig. 2a). These fluctuations suggest the presence of temporal patterns influencing the infection's transmission dynamics. Fig. 6 illustrates the additive time series decomposition of monthly infections. Gonorrhea infections experience a rise from August 2005 to October 2008, reaching a historical peak of 158 infections in September 2007, and a mild increase occur from August 2011 to November 2013 with a peak of 145 infections in August 2012. Additionally, there is a

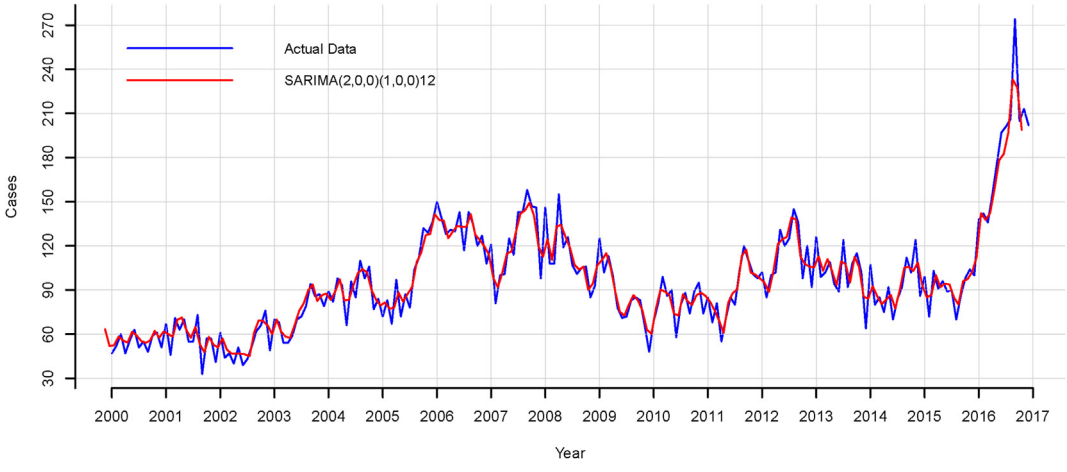


**Fig. 7.** Monthly time series data and SARIMA model fitting.

significant increase in the number of infections from 2015 until the end of the study period in 2016 with a peak of 274 infections in September 2016.

The time series decomposition reveals that Gonorrhea occurrence has a seasonal and recurring patterns over the late summer and fall (Fig. 6) seasons with higher numbers of infections occurring from August through November each year. The Friedman test (Ollech & Webel, 2020) for seasonality is utilized to assess the statistical significance of the existence of the seasonal trend within the dataset. Furthermore, a SARIMA(2, 0, 0)(1, 0, 0)12 model with $\varphi_1 = 0.47$, $\varphi_2 = 0.45$, and $\Phi_1 = 0.17$ is effectively applied (Fig. 7), confirming the presence of a strong temporal trend of infections. We apply a Box-Cox transformation (Box & Cox, 1964) with the parameter estimated at 0.01 before fitting the SARIMA model to make the model variance stationary. The residuals from the fitted SARIMA model demonstrate that they are uncorrelated and normally distributed with a mean of zero and a constant variance. The Ljung-Box test (Ljung & Box, 1978) is employed to investigate the existence of residual autocorrelation subsequent to model fitting. The outcomes of the test reveal that no residual autocorrelation persisted within the fitted model.

### 3.4. Spatio-temporal patterns

We employ a spatial and temporal scanning window size of 50% of the total population at risk and the entire study duration to detect the significant space-time clusters. Additionally, we consider aggregated monthly data of infections across all RHADs from 2000 to 2016 in our spatio-temporal analysis. Kulldorff's space-time scan statistic, applied through a discrete Poisson model within a spatio-temporal framework, reveals space-time heterogeneity in the spread of infections in Manitoba from 2000 to 2016 and identifies the most likely and the secondary statistically significant high-risk clusters illustrated in Fig. 8. The most likely space-time cluster is located in the northern districts of Manitoba including 16 RHADs. This most likely space-time cluster occurs during the high-risk period from January 2006 to June 2014 with 3617 reported infections and a relative risk of 5.3. In addition, the secondary cluster is identified in central districts of Winnipeg, covering 2 RHADs. This secondary space-time cluster is associated with a high-risk period from June 2004 to November 2012, including a total of 1896 reported infections and a relative risk of 2.91.

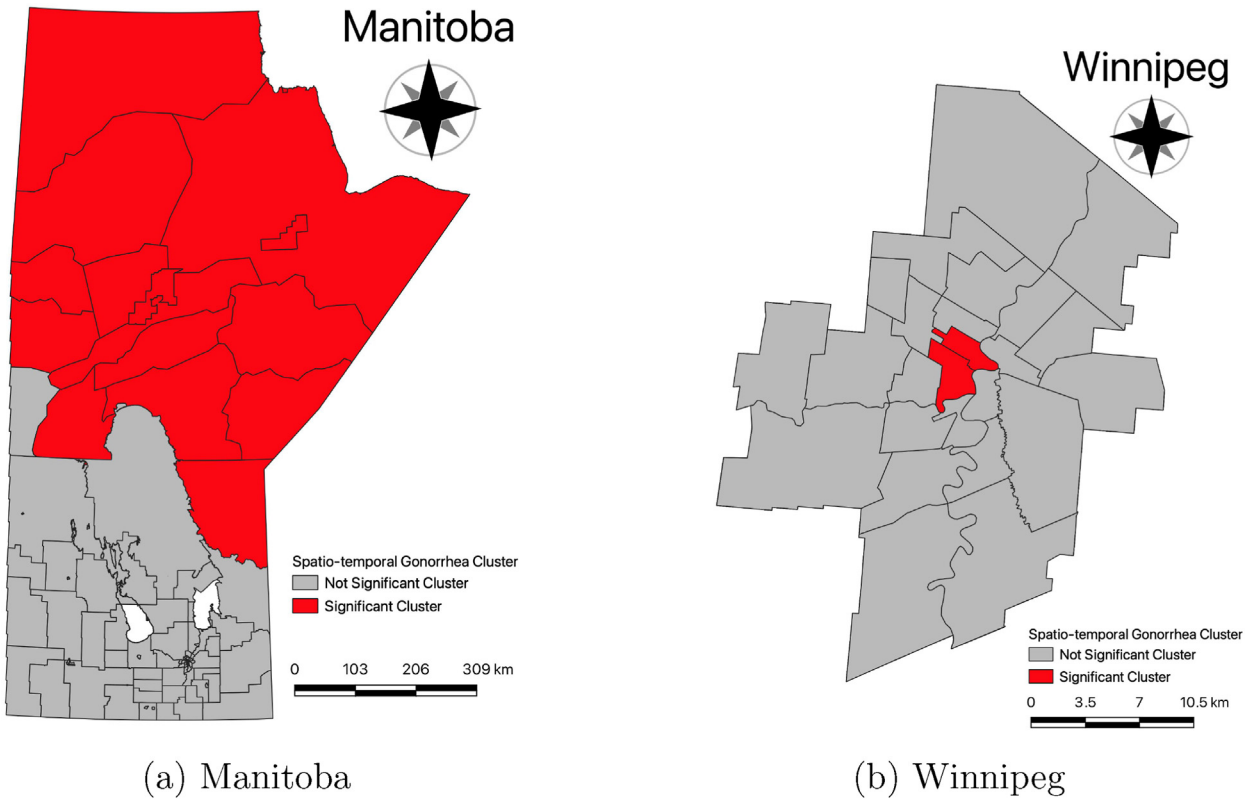


**Fig. 8.** Spatio-temporal clusters of Gonorrhea infections in Manitoba, 2000–2016.

## 4. Discussion

The findings of this study enhance our knowledge of Gonorrhea transmission dynamics, the epidemic, and its spread through space and time in Manitoba. This research investigates the temporal, spatial, and spatio-temporal clusters of the infection at the RHAD level within the Canadian province of Manitoba, from 2000 to 2016. Purely spatial analysis of the infections reveals that there are significant clusters of Gonorrhea in Manitoba, particularly in the northern district of the province with 20 RHADs and the central districts of Winnipeg with 6 RHADs. The temporal analysis of the infections uncovers a seasonal and recurrent pattern, with Gonorrhea infections consistently peaking during the late summer and fall months each year. The spatio-temporal cluster analysis offers additional evidence of RHADs experiencing a higher number of infections than what would be expected within a specified geographic area and time frame. The spatio-temporal analysis shows that the distribution of the infections in Manitoba from 2000 to 2016 exhibits significant spatial and temporal variations. Specifically, high-risk clusters are identified in two distinct periods and geographical locations: the identified high-risk clusters are located in the northern parts of Manitoba from 2006 to 2014 and central districts of Winnipeg from 2004 to 2012. The high-risk cluster located in the northern parts of Manitoba is the larger cluster covering a total of 16 RHADs. Furthermore, there are disparities in reported infections based on sex and age, with a higher incidence among females and a lower mean age compared to males. The higher rates of female cases may be attributed to the fact that Gonorrhea tends to be more asymptomatic in males. Moreover, nearly 16% of the 2016 reported infections are associated with individuals who experienced multiple infections within a single year. Those individuals can significantly contribute to the infection's spread. Therefore, it is essential to identify and address this specific group to minimize the overall transmission of the infection in the community.

This study has some limitations. First, while our administrative data includes all laboratory-confirmed infections in the province, this data is potentially underreported due to the asymptomatic nature of the disease and the healthcare-seeking behaviors of individuals. Second, individual-level data on laboratory-confirmed Gonorrhea infections after 2016 were not accessible during the time of conducting this study. Additionally, due to the lack of data on the sexual behaviors of the infected individuals, we are not able to identify high-risk sexual behaviors which could be informative for the public health officials for the further interventions and prevention strategies.

## 5. Conclusion

To the best of our knowledge, this study is the first investigation into the spatial, temporal, and spatio-temporal clustering of Gonorrhea infection in Manitoba between 2000 and 2016 at the RHAD level, using individual-level, laboratory-confirmed administrative data. This study detects the existence of the temporal, spatial, and spatio-temporal clusters of the infection at the RHAD level. This study also evaluates the variations in the spread of Gonorrhea across different age and sexes within the province. Emphasizing the frequency of repeat Gonorrhea infections can play a crucial role in increasing public awareness about the importance of practicing safe sexual behaviors, getting regular testing, and adhering to prescribed treatments. This heightened awareness has the potential to stimulate behavioral changes that effectively lower the risk of infection.

The outcomes of this study provide valuable insights for public health and Manitoba Health as they reveal the existence of high-risk clusters of Gonorrhea infections. These high-risk clusters determine where the prevention strategies, control measures, and allocation of resources should be focused and strengthened to reduce the burden of the infection. Furthermore, policymakers should prioritize age and sex groups that are at higher risk of both contracting and spreading the infection. This emphasis is essential for the development of targeted and localized prevention strategies and control programs. Given that Gonorrhea is more prevalent among younger age groups, particularly among females, there is a clear need for comprehensive health education programs in schools, colleges, universities, and the general public. These programs should aim to educate individuals about the risks associated with the infection, modes of transmission, available treatments, common symptoms, and the importance of utilizing screening programs and accessing clinical services. This proactive approach is vital in raising awareness and promoting responsible sexual health practices to reduce the spread of Gonorrhea.

## Ethical considerations

The research protocol of the present study was reviewed by and obtained ethical approvals from both the Health Research Ethics Board (HREB) of the University of Manitoba and the Provincial Health Research Privacy Committee (PHRPC) of Manitoba Health.

## CRediT authorship contribution statement

**Amin Abed:** Writing – review & editing, Writing – original draft, Visualization, Validation, Software, Project administration, Methodology, Investigation, Formal analysis, Conceptualization. **Mahmoud Torabi:** Writing – review & editing, Visualization, Supervision, Methodology, Conceptualization. **Zeinab Mashreghi:** Writing – review & editing, Visualization, Supervision, Methodology, Conceptualization.

## Declaration of competing interest

The authors declare that they have no known competing financial interests or personal relationships that could have appeared to influence the work reported in this paper.

## Acknowledgement

The results and conclusions are those of the authors and no official endorsement by the MCHP, Manitoba Health, or other data providers is intended or should be inferred. Data used in this study are from the Population Health Research Data Repository housed at the MCHP, University of Manitoba and were derived from data provided by Manitoba Health. This work was supported by grants from Natural Sciences and Engineering Research Council of Canada (NSERC).

## References

Bernstein, K. T., Marcus, J. L., Nieri, G., Philip, S. S., & Klausner, J. D. (2010). Rectal gonorrhea and chlamydia reinfection is associated with increased risk of HIV seroconversion. *JAIDS Journal of Acquired Immune Deficiency Syndromes, 53*, 537–543.
Blanchard, J. F., Moses, S., Greenaway, C., Orr, P., Hammond, G., & Brunham, R. (1998). The evolving epidemiology of chlamydial and gonococcal infections in response to control programs in Winnipeg, Canada. *American Journal of Public Health, 88*, 1496–1502.
Box, G. E., & Cox, D. R. (1964). An analysis of transformations. *Journal of the Royal Statistical Society - Series B: Statistical Methodology, 26*, 211–243.
Box, G. E., Jenkins, G. M., Reinsel, G. C., & Ljung, G. M. (2015). *Time series analysis: Forecasting and control*. John Wiley & Sons.
Bush, K. R., Henderson, E. A., Dunn, J., Read, R. R., & Singh, A. (2008). Mapping the core: chlamydia and gonorrhea infections in calgary, Alberta. *Sexually Transmitted Diseases*, 291–297.
Cantos, V. D., & del Rio, C. (2020). Gonorrhea in adolescents and young adults. In *Sexually transmitted infections in adolescence and young adulthood: A practical guide for clinicians* (pp. 169–182).
Chan, K. S., & Cryer, J. D. (2008). *Time series analysis with applications in R*. Springer.
Choudhri, Y., Miller, J., Sandhu, J., Leon, A., & Aho, J. (2018). Sexually transmitted infections: Gonorrhea in Canada, 2010–2015. *Canada Communicable Disease Report, 44*, 37.
Davidson, K. W., Barry, M. J., Mangione, C. M., Cabana, M., Caughey, A. B., Davis, E. M., Donahue, K. E., Doubeni, C. A., Krist, A. H., Kubik, M., et al. (2021). Screening for chlamydia and gonorrhea: US preventive services task force recommendation statement. *JAMA, 326*, 949–956.
Faverjon, C., & Berezowski, J. (2018). Choosing the best algorithm for event detection based on the intended application: A conceptual framework for syndromic surveillance. *Journal of Biomedical Informatics, 85*, 126–135.
Fukuda, Y., Umezaki, M., Nakamura, K., & Takano, T. (2005). Variations in societal characteristics of spatial disease clusters: Examples of colon, lung and breast cancer in Japan. *International Journal of Health Geographics, 4*, 1–13.
Hippe, J., & Jolly, A. M. (2012). STI phase and the geography of sexual partnerships: Prevalence of long-distance sexual contacts among chlamydia, gonorrhea, and coinfected STI cases in Manitoba, Canada. *Spatial and spatio-temporal epidemiology, 3*, 255–263.
Holmes, K. K., Sparling, P. F., Stamm, W. E., Piot, P., Wasserheit, J. N., Corey, L., Cohen, M., Watts, D. H., & Nelson, R. A. (2007). *Sexually transmitted diseases*. McGraw-Hill.
Hosenfeld, C. B., Workowski, K. A., Berman, S., Zaidi, A., Dyson, J., Mosure, D., Bolan, G., & Bauer, H. M. (2009). Repeat infection with Chlamydia and gonorrhea among females: A systematic review of the literature. *Sexually Transmitted Diseases*, 478–489.
Kulldorff, M. (1997). A spatial scan statistic. *Communications in Statistics - Theory and Methods, 26*, 1481–1496.
Kulldorff, M., Rand, K., Gherman, G., Williams, G., DeFrancesco, D., & SaTScan, V. (1998). *Software for the spatial and space-time scan statistics*. SaTScan & M. Version 2.
Leichliter, J. S., Dittus, P. J., Copen, C. E., & Aral, S. O. (2020). Trends in factors indicating increased risk for STI among key subpopulations in the United States, 2002–2015. *Sexually Transmitted Infections, 96*, 121–123.
Lenz, J. D., & Dillard, J. P. (2018). Pathogenesis of Neisseria gonorrhoeae and the host defense in ascending infections of human fallopian tube. *Frontiers in Immunology, 9*, 2710.
Lix, L. M., Smith, M., Azimaee, M., Dahl, M., Nicol, P., Burchill, C., Burland, E., & Bailly, A. (2012). *A systematic investigation of Manitoba's provincial laboratory data*. Winnipeg, MB: Manitoba Centre for Health Policy.
Ljung, G. M., & Box, G. E. (1978). On a measure of lack of fit in time series models. *Biometrika, 65*, 297–303.
Lu, D., Strauss, B., Simkus, K., Tepper, M., Gagnon, F., Johnson, N., Girard, E., & Barnes, K. (2020). Adverse events following mass antibiotic prophylaxis during a Group A Streptococcus outbreak in the Canadian Forces Leadership and Recruit School. *Canada Communicable Disease Report= Releve des Maladies Transmissibles au Canada, 46*, 264–271.
Lunny, C., Taylor, D., Hoang, L., Wong, T., Gilbert, M., Lester, R., Krajden, M., & Ogilvie, G. (2015). Self-collected versus clinician-collected sampling for chlamydia and gonorrhea screening: A systemic review and meta-analysis. *PLoS One, 10*, Article e0132776.
Moran, P. A. (1950). Notes on continuous stochastic phenomena. *Biometrika, 37*, 17–23.
Ochsendorf, F. (2008). Sexually transmitted infections: Impact on male fertility. *Andrologia, 40*, 72–75.
Okonofua, F. E., Ntoimo, L. F. C., Omonkhua, A., Ayodeji, O., Olafusi, C., Unuabonah, E., & Ohenhen, V. (2022). Causes and risk factors for male infertility: A scoping review of published studies. *International Journal of General Medicine*, 5985–5997.
Ollech, D., & Webel, K. (2020). *A random forest-based approach to identifying the most informative seasonality tests*.
Pinto, C. N., Dorn, L. D., Chinchilli, V. M., & Du, P. (2018). Chlamydia and gonorrhea acquisition among adolescents and young adults in Pennsylvania: A rural and urban comparison. *Sexually Transmitted Diseases, 45*, 99–102.
Schmale, J. D., Martin, J. E., & Domescik, G. (1969). Observations on the culture diagnosis of gonorrhea in women. *JAMA, 210*, 312–314.
Simms, I., & Stephenson, J. (2000). Pelvic inflammatory disease epidemiology: What do we know and what do we need to know? *Sexually Transmitted Infections, 76*, 80–87.
Trojian, T. H., Lishnak, T. S., & Heiman, D. (2009). Epididymitis and orchitis: An overview. *American Family Physician, 79*, 583–587.
Unemo, M., Ballard, R., Ison, C., Lewis, D., Ndowa, F., Peeling, R., Organization, W. H., et al. (2013). *Laboratory diagnosis of sexually transmitted infections, including human immunodeficiency virus*.
Unemo, M., Seifert, H. S., Hook III, E. W., Hawkes, S., Ndowa, F., & Dillon, J. A. R. (2019). Gonorrhoea. *Nature Reviews Disease Primers, 5*, 79.
Vallely, L. M., Egli-Gany, D., Wand, H., Pomat, W. S., Homer, C. S., Guy, R., Silver, B., Rumbold, A. R., Kaldor, J. M., Vallely, A. J., et al. (2021). Adverse pregnancy and neonatal outcomes associated with Neisseria gonorrhoeae: Systematic review and meta-analysis. *Sexually Transmitted Infections, 97*, 104–111.
van Lier, A., McDonald, S. A., Bouwknegt, M., Kretzschmar, M. E., Havelaar, A. H., Mangen, M. J. J., Wallinga, J., & de Melker, H. E. (2016). Disease burden of 32 infectious diseases in The Netherlands, 2007-2011. *PLoS One, 11*, Article e0153106.
Walker, C. K., & Sweet, R. L. (2011). *Gonorrhea infection in women: Prevalence, effects, screening, and management*. International journal of women's health.

Wang, Y. C., Chung, C. H., Chen, J. H., Chiang, M. H., Tsao, C. H., Lin, F. H., Chien, W. C., Shang, S. T., & Chang, F. Y. (2017). Gonorrhea infection increases the risk of prostate cancer in Asian population: A nationwide population-based cohort study. *European Journal of Clinical Microbiology & Infectious Diseases, 36*, 813–821.
West, M. (1997). Time series decomposition. *Biometrika, 84*, 489–494.
Whelan, J., Abbing-Karahagopian, V., Serino, L., & Unemo, M. (2021). Gonorrhoea: A systematic review of prevalence reporting globally. *BMC Infectious Diseases, 21*, 1–23.
Workowski, K. (2013). Chlamydia and gonorrhea. *Annals of Internal Medicine, 158*.
World Health Organization. (2018). *Report on global sexually transmitted infection surveillance 2018*.